SCINDEKS
Serbian Citation Index
J Med Biochem 2026; 45 DOI: 10.5937/jomb0-64432

UDK 577.1 : 61 **ISSN 1452-8258**

J Med Biochem 45: 1–10, 2026

Original paper
Originalni naučni rad

COMBINED MLH1/MSH2/MSH6 ASSESSMENT BY IHC AND RT-QPCR: DIFFERENTIAL EXPRESSION ANALYSIS AND INCREMENTAL VALUE FOR PATHOLOGICAL RISK STRATIFICATION IN COLORECTAL CANCER

KOMBINOVANA PROCENA MLH1/MSH2/MSH6 POMOĆU IHC I RT-QPCR: ANALIZA DIFERENCIJALNE EKSPRESIJE I INKREMENTALNA VREDNOST ZA STRATIFIKACIJU PATOLOŠKOG RIZIKA KOD KOLOREKTALNOG KARCINOMA

Yi Zhang, Xin Li, Jing Ran, Ningchuan Zuo*

Department of Pathology, Liangjiang Hospital of Chongqing Medical University, Chongqing, 401121, China

Summary

Background: Mismatch repair (MMR) status is routinely assessed in colorectal cancer (CRC), yet the laboratory value of combining multiple MMR targets across platforms for risk stratification requires verification under real-world testing conditions. This study evaluated MutL Homolog 1 (MLH1), MutS Homolog 2 (MSH2) and MutS Homolog 2 (MSH6) using immunohistochemistry (IHC) and RT-qPCR in resection specimens and quantified the added value of combined assessment for stratifying tumor invasion and lymph node status.
Methods: FFPE tumor tissue and paired adjacent non-tumor tissue were collected from patients undergoing radical resection (April 2024–June 2025). IHC was interpreted using internal positive controls and a predefined dichotomous rule (retained vs complete loss in tumor nuclei). RT-qPCR assays were performed with batch-level controls, non-template controls, and replicate measurements; acceptance criteria were prespecified. Agreement between readers and between platforms was assessed. Multivariable logistic models were used to evaluate discrimination for advanced invasion and node-positive disease, with internal validation and calibration assessment.
Results: MLH1, MSH2 and MSH6 were reduced in tumor tissue compared with adjacent tissue at both protein and mRNA levels. Lower MMR expression was associated with more advanced invasion and positive nodal status. A combined model incorporating MLH1/MSH2/MSH6 improved discrimination compared with single markers.

Kratak sadržaj

Uvod: Status popravke neusklađenosti (MMR) se rutinski procenjuje kod kolorektalnog karcinoma (CRC), ali laboratorijska vrednost kombinovanja više MMR ciljeva na različitim platformama za stratifikaciju rizika zahteva verifikaciju u realnim uslovima testiranja. Ova studija je procenila MutL Homolog 1 (MLH1), MutS Homolog 2 (MSH2) i MutS Homolog 2 (MSH6) koristeći imunohistohemiju (IHC) i RT-qPCR u resekcijskim uzorcima i kvantifikovala dodatnu vrednost kombinovane procene za stratifikovanje invazije tumora i statusa limfnih čvorova.
Metode: FFPE tumorsko tkivo i upareno susedno netumorsko tkivo prikupljeni su od pacijenata koji su podvrgnuti radikalnoj resekciji (april 2024–jun 2025). IHC je interpretiran korišćenjem internih pozitivnih kontrola i unapred definisanog dihotomnog pravila (zadržano naspram potpunog gubitka u tumorskim jezgrima). RT-qPCR testovi su sprovedeni sa kontrolama na nivou serije, kontrolama koje nisu šabloni i ponovljenim merenjima; kriterijumi prihvatanja su unapred određeni. Procenjena je saglasnost između čitača i između platformi. Multivarijantni logistički modeli su korišćeni za procenu diskriminacije za uznapredovalu invaziju i bolest pozitivnu na čvorove, sa internom validacijom i procenom kalibracije.
Rezultati: MLH1, MSH2 i MSH6 su bili smanjeni u tumorskom tkivu u poređenju sa susednim tkivom, kako na nivou proteina, tako i na nivou mRNA. Niža ekspresija MMR bila je povezana sa naprednijom invazijom i pozitivnim nodalnim statusom. Kombinovani model koji uključuje MLH1/MSH2/MSH6 poboljšao je diskriminaciju

Address for correspondence:

Dr. Yi Zhang,
Department of Pathology, Liangjiang Hospital of Chongqing Medical University,No. 2 Jinkaida Avenue, Liangjiang New Area, Chongqing, 401121, China
e-mail:cqzy7278@163.com

Quality control metrics supported the feasibility of the combined workflow in routine laboratory settings.
Conclusion: A combined MLH1/MSH2/MSH6 testing strategy integrating IHC and RT-qPCR provides measurable incremental value for pathological risk stratification in CRC when implemented with standardized interpretation and quality control.

Keywords: colorectal cancer, MLH1, MSH2, MSH6, mismatch repair, clinicopathological features, assessment value

u poređenju sa pojedinačnim markerima. Metrike kontrole kvaliteta podržale su izvodljivost kombinovanog toka rada u rutinskim laboratorijskim uslovima.
Zaključak: Kombinovana strategija testiranja MLH1/MSH2/MSH6 koja integriše IHC i RT-qPCR pruža merljivu inkrementalnu vrednost za stratifikaciju patološkog rizika kod kolorektalnog karcinoma kada se implementira sa standardizovanom interpretacijom i kontrolom kvaliteta.

Ključne reči: kolorektalni karcinom, MLH1, MSH2, MSH6, popravka neusklađenosti, kliničko-patološke karakteristike, vrednost procene

Introduction

Among various malignancies, colorectal cancer (CRC) ranks third in morbidity worldwide, with persistently high incidence and mortality rates, posing a substantial global health burden (1). Despite advances in assessment techniques and therapeutic strategies, early detection and accurate risk stratification remain critical determinants of patient prognosis (2). Colorectal cancer is characterized by marked biological heterogeneity. Although the TNM staging system remains the cornerstone of clinical decision-making, it does not fully capture tumor biological behavior or interindividual variability (3). In recent years, defects in the DNA mismatch repair (MMR) system and the resulting microsatellite instability (MSI) have been recognized as key molecular features of CRC, with important implications for prognosis evaluation and therapeutic decision-making (4). *MutL Homolog 1 (MLH1)*, *MutS Homolog 2 (MSH2)* and *MutS Homolog 2 (MSH6)* are core components of the MMR pathway. Loss of their expression is closely associated with the MSI-high (MSI-H) phenotype and has been implicated in tumor invasiveness, chemosensitivity, and response to immunotherapy (5–7). Previous studies have reported associations between MMR status and clinicopathological characteristics in CRC. MSI-H tumors are more frequently observed in early-stage disease (stage I–II) and are generally associated with a lower rate of lymph node metastasis; however, their prognostic significance remains controversial (8). Aberrant *MLH1* promoter methylation represents the predominant mechanism underlying sporadic MSI-H CRC and has been linked to clinical variables such as age and tumor location (9). However, most of the existing studies focus on the expression of a single MMR protein or MSI status. There is still a lack of systematic analysis of the combined expression patterns of *MLH1*, *MSH2*, and *MSH6* and their relationship with pathological progression. In addition, whether combined detection can improve the accuracy of disease assessment, especially in predicting the risk of metastasis and guiding individualized treatment, remains to be validated in large-scale cohorts.

In routine practice, MMR evaluation is frequently performed as part of the pathology–laboratory interface, where analytical robustness, interpretability, and reporting utility are as important as biological association. However, most studies emphasize single-marker interpretation or MSI categorization, while fewer address whether a standardized, combined *MLH1/MSH2/MSH6* workflow – implemented across IHC and RT-qPCR – can provide incremental value for risk stratification beyond conventional staging under real-world laboratory constraints. Therefore, this study assessed *MLH1*, *MSH2* and *MSH6* using a prespecified interpretation framework and quality control procedures, and evaluated whether combined assessment improves discrimination for advanced tumor invasion and lymph node metastasis.

Materials and Methods

Research design

This retrospective cohort study was conducted to evaluate a combined laboratory workflow for *MLH1*, *MSH2* and *MSH6* testing in colorectal cancer. Clinicopathological data and FFPE tissue specimens were collected from patients who underwent radical surgical resection at our hospital between April 2024 and June 2025. The primary objectives were (i) to assess analytical feasibility and interpretation agreement of *MLH1/MSH2/MSH6* testing across IHC and RT-qPCR and (ii) to quantify the incremental value of combined assessment for stratifying tumor invasion and lymph node status.

Sample size estimation

By referring to previous literature (10), we assumed a lymph node metastasis rate of about 35% in CRC patients and a MMR protein loss rate of about 15%. With $\alpha = 0.05$ (two-tailed) and $\beta = 0.2$ (80% power), and using the independent sample comparison analysis in G-Power 3.1 software, it is calculated that at least 147 participants were needed.

Research participants

Inclusion criteria: (1) Pathologically diagnosed primary CRC and treatment with radical resection (with D2 or above lymphadenectomy) after admission, with the invasion depth (T stage) and lymph node metastasis status (N stage) clearly defined by postoperative pathology. T- was defined as carcinoma in situ (Tis) according to the 8th edition of the TNM staging system for colorectal cancer, and T+ was defined as tumor invasion beyond the basement membrane (T1–T4). All cases were re-evaluated by two senior pathologists to ensure the accuracy of T staging. (2) Well-preserved paraffin-embedded samples of tumor and adjacent tissues were (remaining tissues $\geq 1 cm^3$) for subsequent detection. (3) Clinicopathological data (age, sex, tumor location, size, degree of differentiation, etc.) completeness. Exclusion criteria: (1) Metastatic CRC (unknown primary focus or recurrence/metastasis). (2) Preoperative neoadjuvant chemoradiotherapy was excluded because it may induce MMR protein degradation and affect the accuracy of expression detection. (3) Autolysis, necrosis, or immunohistochemical staining failure occurred during the detection of the remaining tissue samples. Ethical approval has been secured from the hospital's Ethics Committee. Informed consent is waived, given the retrospective research design.

IHC staining and interpretation

After deparaffinization and hydration of the paraffin sections, the tissue was subjected to antigen retrieval was performed with citrate buffer (pH6.0) in a pressure cooker at 121 °C for 2 minutes. Subsequently, endogenous peroxidase was blocked by incubation with 3% H_2O_2 at room temperature for 10 minutes. Mouse anti-human *MLH1* (Abcam, ab92312, clone ES05, dilution 1:100), *MSH2* (Abcam, ab1421, clone FE11, dilution 1:200), and *MSH6* (Abcam, ab131038, clone 44, dilution 1:100) primary antibodies were applied for 60 min at room temperature. Antigen retrieval was performed using citrate buffer (pH 6.0) in a pressure cooker at 121 °C for 2 min; the secondary antibody (Dako EnVision kit, K4003) was incubated for 30 min at room temperature. DAB development time was strictly controlled at 5 min for all markers to ensure consistent staining intensity. Paired adjacent non-tumor tissue (defined as tissue ≥2 cm away from the tumor margin without histological evidence of malignancy) served as the control.

Interpretation followed a prespecified dichotomous rule: retained expression was defined as unequivocal nuclear staining in tumor cells with appropriate staining in internal controls; complete loss was defined as absence of nuclear staining in tumor cells with concurrent positive nuclear staining in internal control cells (stromal lymphocytes and/or non-neoplastic epithelium) on the same slide. Slides without interpretable internal controls or with technical failure were classified as non-evaluable and excluded from downstream modeling. Two senior pathologists independently reviewed all slides while blinded to clinical data; discordant cases were resolved by joint review, and reader agreement was quantified (κ statistic) as part of the analytical assessment. After binary classification of retained/complete loss, the positive expression rate of tumor cells was further calculated as a continuous variable (mean ± SD) by counting 5 random high-power fields (×400) per section, to quantify the expression level of MMR proteins in positive cases. For IHC staining, slides with non-interpretable internal controls or staining artifacts were classified as non-evaluable and excluded (n = 8). For FFPE RNA extraction, samples with A260/A280 ratio outside 1.8–2.0 were excluded (n = 12).

RT-qPCR

RT-qPCR experiments and data analysis were performed in a blinded manner. The researchers were unaware of the pathological outcomes (e.g., T staging, lymph node metastasis status) of the samples during RNA extraction, reverse transcription, and qPCR detection. Total RNA was extracted from FFPE tissues using Trizol reagent kit with on-column DNase treatment. RNA quantity and purity were assessed by spectrophotometry (A260/A280 and A260/A230). Given the fragmented nature of FFPE RNA, integrity assessment relied on assay performance metrics rather than rRNA band visualization. Reverse transcription was performed using [reverse transcription kit] with defined RNA input ([ng/μg]). RT-qPCR was run in technical duplicates with non-template controls and no–reverse-transcription controls in each batch. Amplicon specificity was verified by single-peak melting curves. Primer sequences are provided in *Table I* (all sequences correspond to experimentally used primers and were confirmed by in silico specificity checks). PCR efficiency for each target was evaluated using a standard dilution series and required to fall within 90%; batches not meeting acceptance criteria were repeated. Relative expression was calculated using the $2^{-\Delta\Delta}Ct$ method with GAPDH as the reference gene. For the $2^{-\Delta\Delta}Ct$ method, the calibrator was defined as paired adjacent non-tumor tissue of each sample. Ct values of technical duplicates were averaged first; samples with Ct value variation>0.5 between duplicates were excluded. $^{\Delta}Ct$ was calculated as Ct (target gene) - Ct (GAPDH), and $^{\Delta\Delta}Ct$ was calculated as $^{\Delta}Ct$ (tumor tissue) - $^{\Delta}Ct$ (adjacent tissue). Technical duplicates were performed for each sample; Ct values with a CV > 5% were excluded, and the experiment was repeated. Only Ct values with CV ≤ 5% were averaged for subsequent ΔCt calculation. Batches

Table I Sequence of the primers.

	F (5′-3′)	R (5′-3′)	bp
MLH1	ATGAGCGCTTCTCCTCCTCT	TCAGGCTCCAGAGTCTTGAA	198
MSH2	GAGGAGGATGCTGAAGAAGG	TCTGCTGCTGCTGCTGTTCT	152
MSH6	CAGCAGCAGCAGCAGCAGCA	TGTTGTTGTTGTTGTTGTTGC	184
GAPDH	ACCACAGTCCATGCCATCAC	TCCACCACCCTGTTGCTGTA	100

with qPCR amplification efficiency outside the range of 90%–110% were discarded and re-tested.

Chemiluminescence immunoassay

Serum samples were centrifuged (3000 rpm, 10 minutes) for supernatant collection. After the instrument was powered on for self-checking, the reagent kits were loaded (ensuring correct carrier positions of magnetic particles, enzyme-labeled antibodies, and substrates), and the detection items (CEA/CA19-9/CA242) were selected. Calibration standards were used to establish a standard curve (6-point calibration), and the quality control samples were tested under control conditions (with a CV <10%). The sample rack was placed with the serum samples to be tested (≤50 μL per sample), and the instrument automatically aspirated the samples to complete the immune reaction, magnetic separation, washing, and luminescence detection. CEA/CA19-9/CA242 concentrations were automatically converted based on the standard curve. During each test, three quality control samples at high, medium, and low concentrations were run simultaneously. The results of 20 consecutive tests were plotted on a Levey-Jennings control chart, with the allowable range being ±2SD.

Quality control

Sample quality control: Tumor tissue sections were screened to avoid necrotic, hemorrhagic, and edge-compressed areas; only regions with uniformly distributed tumor cells and moderate density were selected for detection. Paraffin-embedded samples were stored at 4 °C in a dry environment to prevent degradation. Given the fragmented nature of FFPE RNA, the main assessment of RNA integrity relied on assay performance metrics (e.g., amplification efficiency ≥90%). 1% agarose gel electrophoresis was used as an auxiliary method only for samples with relatively high RNA quality, and the 28S/18S ratio ≥1.8 was a reference index rather than a mandatory criterion. RNA purity was confirmed by Nanodrop 2000, with A260/A280 ratios strictly controlled between 1.8 and 2.0.

Detection method quality control: For IHC staining, mouse anti-human *MLH1* (Abcam, ES05), *MSH2* (Abcam, FE11), and *MSH6* (Abcam, 44) antibodies were used, with specificity verified by the manufacturer's technical specifications (no cross-reactivity with other proteins). Negative controls (without primary antibody) and positive controls (known MMR-proficient CRC tissues) were set up simultaneously. For qPCR, primers were designed via Primer3 and validated by BLAST, showing no non-specific binding to other human genes; melting curve analysis confirmed a single peak for each amplicon, ensuring product specificity. For chemiluminescence immunoassay (Mindray CL-6000i), high-, medium-, and low-concentration quality control samples were tested in parallel with each batch of samples, with CV <10% (high-concentration CV: 3.2%–5.8%, medium-concentration CV: 4.1%–6.3%, low-concentration CV: 5.3%–8.7%). Results of 20 consecutive tests were plotted on Levey-Jennings control charts, and tests were repeated if results exceeded ±2SD.

Result interpretation quality control: IHC slides were reviewed by two senior pathologists in a double-blind manner. For inconsistent judgments, a third senior pathologist was consulted to reach a consensus. Positive cell counting was performed by selecting 5 random high-power fields (×400) per section, and the average positive rate was calculated to reduce sampling bias.

Statistical analysis

SPSS 26.0 software was used for all statistical analyses. Normality of continuous data was assessed using the Shapiro-Wilk test, and variance homogeneity was verified by Levene's test. Chi-square tests were used for the comparisons of counting data [n(%)]; measurement data ($\bar{\chi}\pm s$) of paired tumor and adjacent tissues were compared by paired sample t-tests; comparisons between different clinical subgroups were performed by independent sample t-tests. Dssessment value analysis was performed with ROC curves, and the joint Logistic model was used for joint detection. The linear predictor was used to distinguish tumor and adjacent tissues, and its optimal cut-off was determined by the maximum Youden index of the ROC curve. Statistical significance is present when $P<0.05$.

Results

Qualitative analysis of MLH1, MSH2, and MSH6

Figure 1 displays the IHC staining results of *MLH1*, *MSH2*, and *MSH6* in cancer and paired adjacent non-tumor tissue of CRC patients. The three MMR proteins dominantly showed negative expression in cancer tissues but were positively expressed in adjacent tissues. Microscopic counting indicated that the positive rates of *MLH1*, *MSH2*, and *MSH6* in CRC tissues were (11.01±3.52)%, (10.62±3.38)%, and (15.78±3.81)%, respectively, which were down-regulated compared to adjacent tissues (P<0.05). About 37.41% (n=55) of the cases showed expression loss of the three proteins, 36.73% (n=54) had absent expression of two proteins, and 25.85% (n=38) exhibited expression loss of a single protein (*Figure 1*).

Quantitative analysis results of MLH1, MSH2, and MSH6

Based on PCR findings, the *MLH1*, *MSH2*, and *MSH6* mRNA expression levels in cancer tissues were (1.50±0.34), (1.29±0.35), and

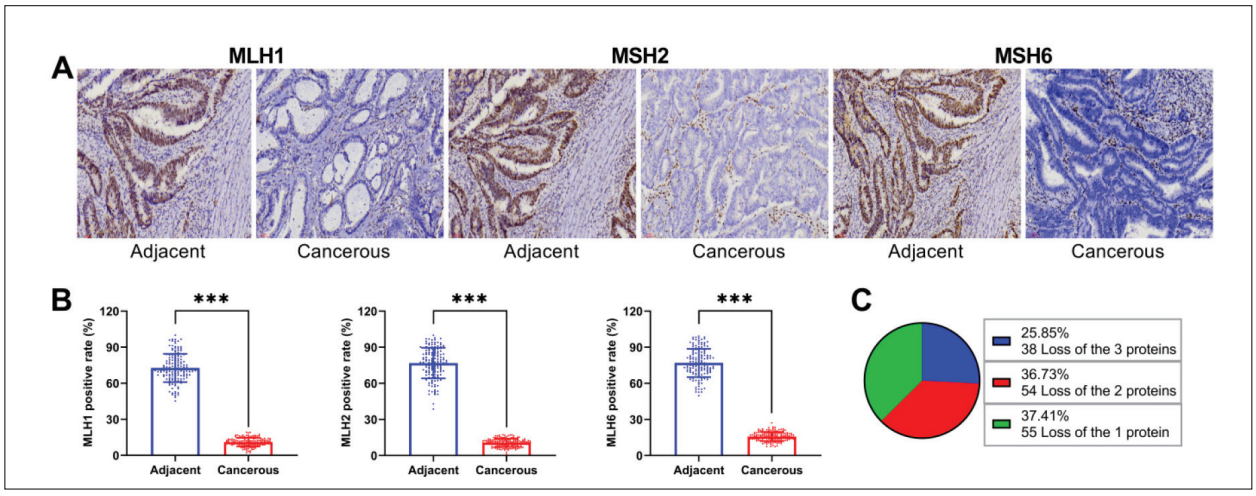

Figure 1 Immunohistochemical (IHC) Staining of MLH1, MSH2, and MSH6 in Colorectal Cancer Tissues.
(A) Representative IHC staining of MLH1, MSH2, and MSH6 in cancer tissues and adjacent tissue. (B) Quantitative analysis of positive expression rates. (C) Distribution of MMR protein loss patterns. ***P<0.001.

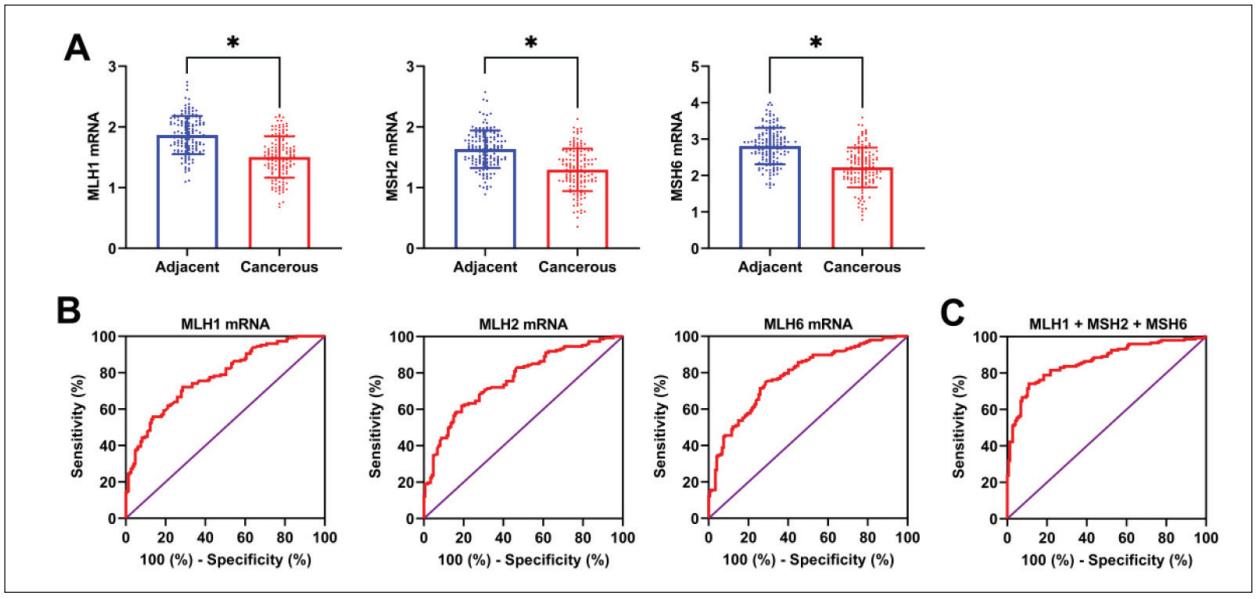

Figure 2 ROC Curves for *MLH1, MSH2, MSH6*, and Combined Detection in CRC Assessment.
(A) Comparison of *MLH1, MSH2*, and *MSH6* expression in cancer tissues and adjacent tissue. (B) ROC curves of *MLH1, MSH2,* and *MSH6* for differential expression analysis between tumor and adjacent tissues and pathological risk stratification of CRC. (C) ROC curve of combined detection of *MLH1, MSH2*, and *MSH6* for the assessment of CRC. *P<0.05.

Table II Differential expression efficacy of MLH1, MSH2, and MSH6 between CRC tumor and adjacent tissues.

	Cut-off	AUC	95%CI	Sensitivity (%)	Specificity (%)	P
MLH1	<1.681	0.778	0.726–0.829	72.11	71.43	<0.001
MSH2	<1.389	0.766	0.712–0.819	61.90	80.95	<0.001
MSH6	<2.567	0.784	0.733–0.836	74.83	71.43	<0.001
Combined detection	>0.581	0.864	0.822–0.906	74.15	89.12	<0.001

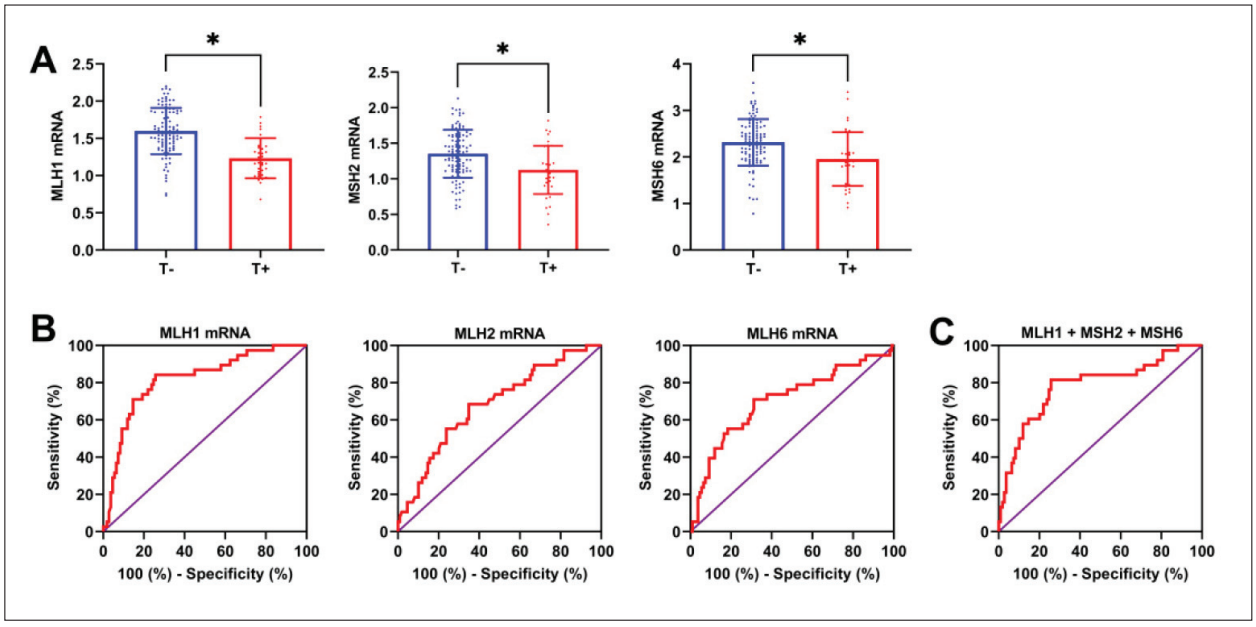

Figure 3 ROC Curves for *MLH1, MSH2, MSH6,* and Combined Detection in Predicting Tumor Invasion (T+).
(A) Comparison of *MLH1, MSH2,* and *MSH6* expression in T − and T+. (B) ROC curves of *MLH1, MSH2,* and *MSH6* for assessment of T+. (C) ROC curve of combined detection of *MLH1, MSH2,* and *MSH6* for assessment of T+. *P<0.05.

Table III Differential expression efficacy of MLH1, MSH2, and MSH6 between (T+) an(T-) tissues.

	Cut-off	AUC	95%CI	Sensitivity (%)	Specificity (%)	P
MLH1	<1.425	0.782	0.691–0.874	81.58	74.31	<0.001
MSH2	<1.221	0.681	0.583–0.779	68.42	65.14	<0.001
MSH6	<2.097	0.704	0.601–0.807	71.05	68.81	<0.001
Combined detection	>0.873	0.817	0.737–0.897	84.21	74.31	<0.001

(2.22±0.54), respectively, which were also lower than those in adjacent tissues (P<0.05). ROC curve analysis showed an AUC of 0.778 for *MLH1* mRNA, 0.764 for *MSH2* mRNA, and 0.763 for *MSH6* mRNA in distinguishing CRC tumor tissues from adjacent non-tumor tissues. Through Logistic regression analysis, a combined detection formula of 11.149+(-2.226×MLH1)+(-2.185×MSH2)+(-1.1608×MSH6) for *MLH1, MSH2,* and *MSH6* was established. This model achieved an enhanced AUC (0.864) for differential expression analysis between tumor and adjacent tissues and pathological risk stratification of CRC, with 74.15% sensitivity and 89.12% specificity (P<0.05) (*Figure 2* and *Table II*).

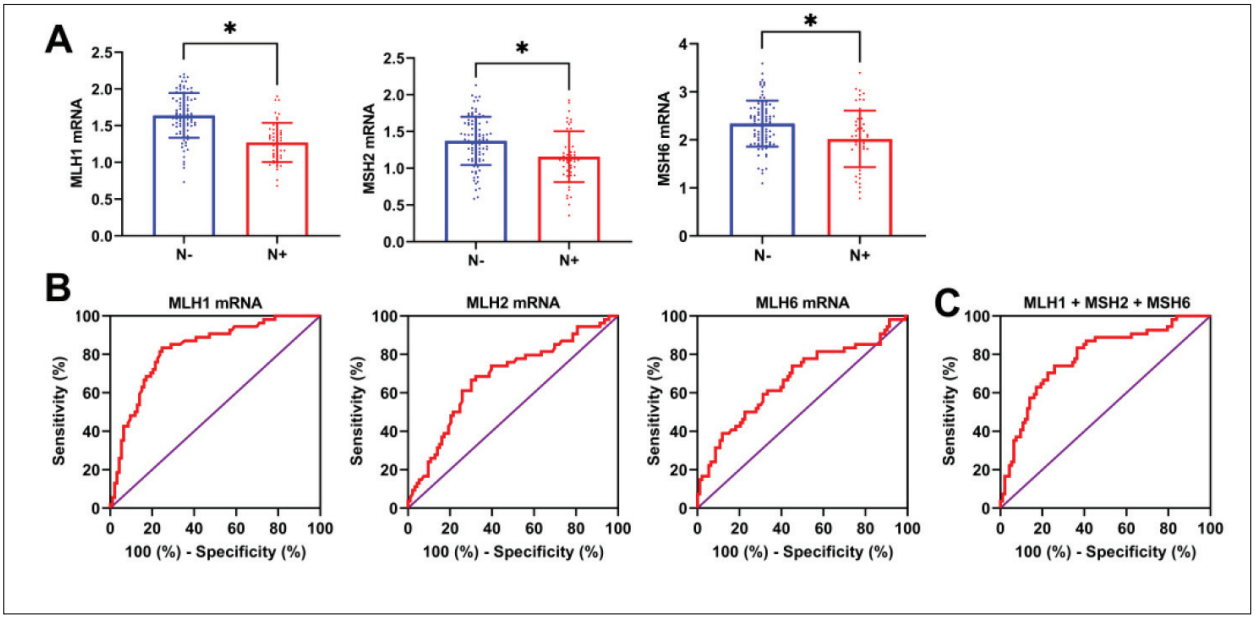

Figure 4 ROC Curves for *MLH1, MSH2, MSH6,* and Combined Detection in Predicting Lymph Node Metastasis (N+). (A) Comparison of *MLH1, MSH2,* and *MSH6* expression in N − and N+. (B) ROC curves of *MLH1, MSH2,* and *MSH6* for assessment of N+. (C) ROC curve of combined detection of *MLH1, MSH2,* and *MSH6* for assessment of N+.

Table IV Differential expression efficacy of MLH1, MSH2, and MSH6 between (N+) an(N-) tissues.

		AUC	95%CI	Sensitivity (%)	Specificity (%)	P
MLH1	<1.433	0.785	0.707–0.862	74.07	74.19	<0.001
MSH2	<1.221	0.681	0.590–0.772	66.67	69.89	<0.001
MSH6	<2.327	0.668	0.574–0.762	74.07	54.84	<0.001
Combined detection	>0.771	0.826	0.757–0.894	83.33	75.27	<0.001

Correlation of MLH1, MSH2, and MSH6 with invasion depth

Pathological biopsy results confirmed carcinoma in situ (T-) in 109 patients. Those with tumor invasion (T+) exhibited lower *MLH1* (1.23±0.27 vs 1.60±0.31), *MSH2* (1.13±0.34 vs 1.35±0.34), and *MSH6* (1.96±0.58 vs 2.31±0.50) levels than patients with T- (P<0.05). As demonstrated by ROC curves, the AUC of the combined detection (*MLH1*+*MSH2*+*MSH6*) for diagnosing T+ was 0.817, corresponding to 84.21% sensitivity and 74.31% specificity (*Figure 3* and *Table III*).

Association of MLH1, MSH2, and MSH6 with lymph node metastasis

In our cohort, 54 patients tested positive for lymph node metastasis (N+). Compared to those with negative lymph node metastasis (N-), the *MLH1* (1.27±0.27 vs 1.64±0.30), *MSH2* (1.16±0.35 vs 1.37±0.33), and *MSH6* (2.02±0.59 vs 2.34±0.48) levels of N+ patients were further decreased (P<0.05). The joint detection by *MLH1, MSH2,* and *MSH6* showed assessment sensitivity and specificity of 83.33% and 75.27% for N+, respectively, outperforming single marker-based assessment (AUC=0.826, P<0.05) (*Figure 4* and *Table IV*).

MLH1, MSH2, and MSH6 correlations with tumor markers

Correlation analysis revealed an inverse correlation of MLH1, MSH2, and MSH6 with tumor markers (CEA, CA19-9, and CA242) in CRC. That is to say, the higher the tumor markers, the lower the levels of MLH1, MSH2, and MSH6 (*Figure 5* and *Table V*).

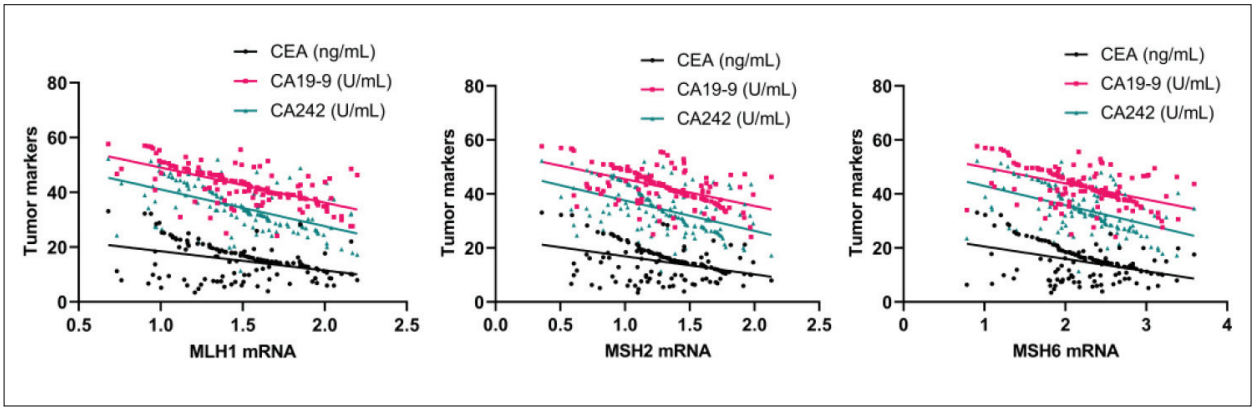

Figure 5 Correlation between MMR Protein Expression and Tumor Markers (CEA, CA19-9, CA242).

Table V Correlation Between MMR Protein Expression and Tumor Markers (CEA, CA19-9, CA242).

	MLH1 mRNA	MSH2 mRNA	MSH6 mRNA
CEA	-0.386	-0.653	-0.563
CA19-9	-0.379	-0.524	-0.488
CA242	-0.404	-0.485	-0.479

Discussion

This study evaluated a combined *MLH1/MSH2/MSH6* testing strategy implemented across IHC and RT-qPCR in CRC resection specimens and examined its utility for pathological risk stratification. The principal findings were: (i) *MLH1, MSH2* and *MSH6* were reduced in tumor tissue compared with paired adjacent tissue at both protein and mRNA levels; (ii) lower MMR expression was associated with more advanced invasion and node-positive status; and (iii) a combined model incorporating multiple MMR targets provided better discrimination than single-marker approaches. Importantly, the workflow was framed as a laboratory procedure with prespecified interpretation rules and batch-level quality control, aligning with practical implementation in a clinical laboratory setting.

Existing evidence has confirmed the central role of MMR proteins (*MLH1, MSH2, MSH6*) in DNA MMR, with MMR functional defects inducing MSI-H and genomic instability (11). This study unveiled lower expression of MMR proteins in cancer tissue compared to adjacent tissues, consistent with previous research findings (12, 13). In addition, we observed that the expression levels of MMR proteins were negatively correlated with the depth of tumor invasion (T staging), which suggests that MMR dysfunction may be associated with enhanced local tumor invasion, potentially through pathways related to DNA damage repair and genomic instability. Potential mechanisms may involve weakened DNA damage repair and genome instability, but specific signaling pathways (e.g., PI3K/AKT/mTOR) require further verification by in vitro experiments (e.g., cell line transfection and Western blot analysis of pathway proteins) (14). Additionally, MMR protein absence may affect the expression of epithelial-mesenchymal transition (EMT)-related genes through epigenetic regulation (15), thus enhancing tumor cells' invasion potential. Notably, this study found a negative relationship between MMR proteins and tumor markers CEA and CA19-9. Of these, CEA has been confirmed to be closely related to CRC invasiveness (16), further supporting that MMR deficiencies are inversely correlated with tumor markers linked to metabolic reprogramming, suggesting a potential association with tumor progression.

From a laboratory perspective, the incremental value of combined assessment is plausible for two reasons. First, IHC and RT-qPCR capture partially overlapping, non-identical sources of variability: IHC is sensitive to fixation, antigen retrieval, and interpretive thresholds, whereas RT-qPCR is influenced by RNA fragmentation and reverse transcription efficiency in FFPE tissues. Integrating multiple targets across platforms can mitigate single-assay limitations and reduce the chance that borderline results drive misclassification. Second, the use of standardized interpretation anchored by internal positive controls (for IHC) and predefined acceptance criteria (for RT-qPCR) supports reproducibility and facilitates structured reporting.

Furthermore, MMR protein levels showed a connection with lymph node metastasis (N staging). In this study, *MLH1, MSH2*, and *MSH6* levels were further reduced in N+ patients compared with N- cases. Besides, their combined detection outperformed single-index detection in assessment

efficiency for N+. Our finding that combined *MLH1/MSH2/MSH6* loss is associated with lymph node metastasis differs from the traditional view that MSI-H CRC has a lower metastasis rate (17). This discrepancy may be attributed to three factors: (1) The present study focuses on the combined loss of three core MMR proteins, while most previous studies analyzed single-protein loss or MSI status (18). (2) The study population in our cohort has distinct clinical and pathological features (e.g., tumor location, differentiation grade) compared to prior cohorts (19). (3) The integrated detection of IHC and RT-qPCR in our study captures both protein and mRNA levels, providing a more comprehensive assessment of MMR function than single-platform testing. Future multicenter studies with larger sample sizes are needed to validate this observation (20). What's more, this study found that MMR proteins were inversely correlated with CA242, a gene whose high expression was closely related to peritoneal metastasis in CRC (21), further suggesting that MMR deficiencies may promote metastasis by down-regulating adhesion molecules.

Considering the relatively small sample size of subgroups, we used cross-validation to evaluate the model performance, which confirmed that the combined model had good generalization ability and low overfitting risk (The average AUC of cross-validation was 0.792 for T+ and 0.801 for N+, which indicated good stability of the model). These results may be relevant to the pathology–laboratory interface where additional, standardized laboratory information is used to complement conventional staging. Rather than replacing TNM staging, a combined *MLH1/MSH2/MSH6* assessment could be reported as an adjunctive risk stratification element, particularly when pathology and laboratory teams seek consistent rules for interpretation and communication. In this context, the combined model's performance should be interpreted together with calibration and internal validation, as discrimination alone does not ensure reliable risk estimates across patient subgroups.

Several limitations should be acknowledged. The study was conducted at a single center, and external validation in an independent cohort is required before broader implementation. Preanalytical variables (e.g., fixation duration and ischemic time) were not fully captured and may affect both IHC and RT-qPCR results. In addition, the panel did not include PMS2, which could lead to incomplete characterization of MMR alterations. Finally, the combined model should be assessed prospectively to confirm whether its use improves clinical decision-making or resource allocation in routine practice. In addition, although PMS2 is also an important MMR protein, its expression is often dependent on *MLH1*, and the combined detection of *MLH1/MSH2/MSH6* can cover most MMR-deficient cases in clinical practice. The incremental value of this panel is that it integrates IHC and RT-qPCR platforms, which provides complementary information at the protein and mRNA levels. Future studies will expand the sample size and include PMS2 to further improve the MMR detection system.

Conclusion

A combined *MLH1/MSH2/MSH6* assessment integrating IHC and RT-qPCR is feasible under a standardized quality-controlled workflow and is associated with advanced invasion and node-positive status in colorectal cancer. Compared with single markers, combined assessment improves stratification performance and may serve as an adjunctive laboratory component to support pathological risk assessment.

Availability of data and materials

The data used to support the findings of this study are available from the corresponding author upon request.

Funding

No funds, grants, or other support was received.

Acknowledgements

Not applicable.

Conflict of interest statement

All the authors declare that they have no conflict of interest in this work.

References

1. Baidoun F, Elshiwy K, Elkeraie Y, Merjaneh Z, Khoudari G, Sarmini MT, et al. Colorectal Cancer Epidemiology: Recent Trends and Impact on Outcomes. Curr Drug Targets 2021; 22(9): 998–1009.
2. Jocić M, Arsenijević N, Gajović N, Jurišević M, Jovanović I, Jovanović M, et al. Anemia of inflammation in patients with colorectal cancer: Correlation with interleukin-1, interleukin-33 and galectin-1. J Med Biochem 2022; 41(1): 79–90.
3. Abedizadeh R, Majidi F, Khorasani HR, Abedi H, Sabour D. Colorectal cancer: a comprehensive review of carcinogenesis, diagnosis, and novel strategies for classified treatments. Cancer Metastasis Rev 2024; 43(2): 729–53.
4. Taieb J, Svrcek M, Cohen R, Basile D, Tougeron D, Phelip JM. Deficient mismatch repair/microsatellite unstable colorectal cancer: Diagnosis, prognosis and treatment. Eur J Cancer 2022; 175: 136–57.
5. Gao Q, Yang L, Ye S, Mai M, Liu Y, Jiang X, et al. Targeting SIRT2 induces MLH1 deficiency and boosts antitumor immunity in preclinical colorectal cancer models. Sci Transl Med. 2025; 17(807): eadv0766.
6. Wu F, Wang X, Zhang H. ŠResearch progress on pathogenic germline mutations in malignant tumorsĆ. Zhonghua Yi Xue Yi Chuan Xue Za Zhi. 2024; 41(12): 1508–15.
7. Graur F, Puia A, Mois E, Pop P, Berar M, Elisei R, et al. Analysis of the MLH1, MLH2, MLH6, PMS2 genes and their correlations with clinical data in rectal mucinous adenocarcinoma. Ann Ital Chir 2022; 93: 188–94.
8. Fan A, Wang B, Wang X, Nie Y, Fan D, Zhao X, et al. Immunotherapy in colorectal cancer: current achievements and future perspective. Int J Biol Sci. 2021; 17(14): 3837–49.
9. Akcay IM, Celik E, Agaoglu NB, Alkurt G, Kizilboga Akgun T, Yildiz J, et al. Germline pathogenic variant spectrum in 25 cancer susceptibility genes in Turkish breast and colorectal cancer patients and elderly controls. Int J Cancer 2021; 148(2): 285–95.
10. Chen S, Ning W, Zhang J, Wu Z, Zhou H, Liu Y. Serum CA19-9 and CEA levels, serum CAT, GSH, oxidised glutathione levels, 8-dihidro-2'-deoksiguanosina and F2-isoprostanes levels in colorectal cancer patients and Lactobacillus: A randomised double-blind controlled trial. J Med Biochem 2025; 44(7): 1440–8.
11. Bartley AN, Mills AM, Konnick E, Overman M, Ventura CB, Souter L, et al. Mismatch Repair and Microsatellite Instability Testing for Immune Checkpoint Inhibitor Therapy: Guideline From the College of American Pathologists in Collaboration With the Association for Molecular Pathology and Fight Colorectal Cancer. Arch Pathol Lab Med 2022; 146(10): 1194–210.
12. Brooksbank K, Martin SA. DNA mismatch repair deficient cancer - Emerging biomarkers of resistance to immune checkpoint inhibition. Int J Biochem Cell Biol 2023; 164: 106477.
13. Rosca OC, Vele OE. Microsatellite Instability, Mismatch Repair, and Tumor Mutation Burden in Lung Cancer. Surg Pathol Clin 2024; 17(2): 295–305.
14. Wang Z, Wang X, Xu Y, Li J, Zhang X, Peng Z, et al. Mutations of PI3K-AKT-mTOR pathway as predictors for immune cell infiltration and immunotherapy efficacy in dMMR/MSI-H gastric adenocarcinoma. BMC Medicine 2022; 20(1): 133.
15. Mikula M, Najjar S, El Jabbour T, Dalvi S, Umrau K, Li H, et al. Increased Cytoplasmic Yes-associated Protein (YAP) Expression in Mismatch Repair Protein-Proficient Colorectal Cancer With High-grade Tumor Budding and Reduced Autophagy Activity. Appl Immunohistochem Mol Morphol 2021; 29(4): 305–12.
16. Cai M, He H, Hong S, Weng J. Synergistic diagnostic value of circulating tumor cells and tumor markers CEA/CA19-9 in colorectal cancer. Scandinavian Journal of Gastroenterology 2023; 58(1): 54–60.
17. Li J, Wu C, Hu H, Qin G, Wu X, Bai F, et al. Remodeling of the immune and stromal cell compartment by PD-1 blockade in mismatch repair-deficient colorectal cancer. Cancer Cell 2023; 41(6): 1152–69 e7.
18. Bateman AC. DNA mismatch repair protein immunohistochemistry - an illustrated guide. Histopathology 2021; 79(2): 128–38.
19. Hou W, Zhao Y, Zhu H. Predictive Biomarkers for Immunotherapy in Gastric Cancer: Current Status and Emerging Prospects. Int J Mol Sci 2023; 24(20).
20. Offermans K, Jenniskens JCA, Simons C, Samarska I, Fazzi GE, van der Meer JRM, et al. Association between mutational subgroups, Warburg-subtypes, and survival in patients with colorectal cancer. Cancer Med 2023; 12(2): 1137–56.
21. Bjorkman K, Mustonen H, Kaprio T, Kekki H, Pettersson K, Haglund C, et al. CA125: A superior prognostic biomarker for colorectal cancer compared to CEA, CA19-9 or CA242. Tumour Biol 2021; 43(1): 57–70.

Recieved: December 23, 2025
Accepted: February 10, 2026